ARTICLE

OBC
www.rsc.org/obc

Theoretical study of the *o*-OH participation in catechol ester ammonolysis

Miroslav A. Rangelov,[a] Georgi N. Vayssilov,[b] Vihra M. Yomtova[a] and Dimiter D. Petkov*[a]

[a] *Laboratory of BioCatalysis, Institute of Organic Chemistry, Bulgarian Academy of Sciences, Sofia, 1113, Bulgaria. E-mail: dd5kov@orgchm.bas.bg*

[b] *Faculty of Chemistry, University of Sofia, Sofia, 1126, Bulgaria. E-mail: gnv@chem.uni-sofia.bg*

Received 12th November 2004, Accepted 11th January 2005
First published as an Advance Article on the web 3rd February 2005

The possible catalytic effect of the vicinal hydroxyl group during the ammonolysis of acetylcatechol has been studied by first principle calculations. A very efficient intramolecular catalysis was found to occur when the catechol ester *o*-OH group is deprotonated: the activation energy of the ammonolysis decreases by 24 kcal mol^{-1} as compared to that of acetylphenol ammonolysis. Using this value, the *o*-oxyanion-catalysed intramolecular ammonolysis was estimated to be orders of magnitude faster than the ammonolysis of acetylphenol or nonionised acetylcatechol. The analogy with the aminolysis of peptidyl-tRNA that occurs during protein biosynthesis implies several orders of magnitude acceleration due to complete or partial deprotonation of its 3′-terminal adenosine 2′-OH providing a mechanistic possibility for general acid–base catalysis by the ribosome.

1 Introduction

Although the *cis*-1,2-diol grouping plays a crucial role in RNA catalysis, our understanding of the specific chemical basis of its catalytic contribution is still fragmentary. The *cis*-2′/3′-diol system of bonded or internal guanosine is a powerful nucleophile or good leaving group in RNA splicing[1] and the 3′-terminal adenosine *cis*-2′/3′-diol is a chemical determinant of peptidyl tRNA reactivity in ribosomal peptide bond synthesis.[2] The aminolysis of *cis*-1,2-diol monoester and nonribosomal aminolysis of peptidyl tRNA, however, have never been probed experimentally since they proceed at an excessively slow rate.[3] On the other hand, monoesters of 1,2-benzenediol (catechol) are known to aminolyse abnormally rapidly.[4–6] We, therefore, studied computationally the catechol ester ammonolysis as a first step towards understanding the key role of the *cis*-2-diol system in RNA catalysis.

Quite recently Sievers *et al.*[7] compared the measured activation parameters for ester aminolysis in the ribosome and in solution and on the basis of a small difference in the activation enthalpy came to the conclusion that "general acid–base catalysis does not play a significant role in peptidyl transfer in the ribosome". Their reference reaction (ester aminolysis by tris(hydroxymethyl)aminomethane) (TRIS), however, is not congruent to the ribosome ester aminolysis reaction. Unlike the aminolysis by amino acid amides, the aminolysis by TRIS proceeds *via* NH_2-general base catalysed alcoholysis by a vicinal OH group, followed by O–N acyl group migration in the resulting TRIS ester[8] to form the final TRIS amide. Therefore, the results of Sievers *et al.*[7] provide support for the involvement of general acid–base catalysis in ribosome catalysis rather than for its absence.

We report here that complete or partial deprotonation of the adjacent hydroxy group of the acetylcatechol ester gives rise to orders-of-magnitude acceleration of the ammonolysis, which suggests an intramolecular general base catalysis by the adjacent *o*-oxyanion. These results are consistent with the kinetic data we have recently reported for catechol ester aminolysis in organic media.[6]

2 Results

2.1 Reaction paths

Previous studies[9] of ester ammonolysis/aminolysis in vacuum or aprotic media have shown that the formation of a zwitterionic tetrahedral intermediate after the initial nucleophilic attack of NH_3/NH_2R on the C=O group is disfavoured. Therefore, we considered the stepwise and the concerted reaction mechanisms only that do not involve such an intermediate.

The stepwise mechanism (lower path in Scheme 1) involves formation of a tetrahedral intermediate **I**, resulting from the association of NH_3 and the carbonyl bond of the catechol ester. The transition state **TS1** results from a nucleophilic attack of the ammonia nitrogen on the carbonyl carbon and simultaneous transfer of one of its hydrogen atoms to the carbonyl oxygen (O_c in Scheme 1). The second transition state **TS2**, involves a proton transfer from the intermediate O_cH to the former ester oxygen O_e, cleavage of the former ester bond C–O_e and restoration of the carbonyl bond C=O_c. Due to the low energy of the rotational transition states[10,11] between the conformers of the intermediates in similar systems, about an order of magnitude lower than the "reaction" transition states, we assume that the former states do not influence the kinetics of the reaction and hence, are not considered.

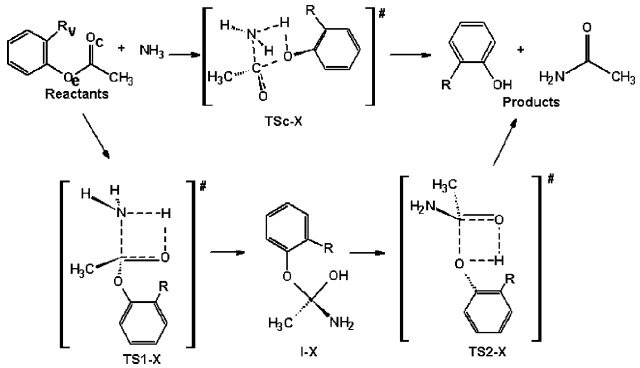

Scheme 1 Reaction mechanisms for ammonolysis of acetylphenol (R = H; X = Ph) and acetylcatechol (R = OH, X = cat).

The concerted reaction (higher path in Scheme 1) proceeds in one step *via* the transition state **TSc**. Like the first step of the stepwise mechanism, the concerted mechanism involves a nucleophilic attack of the ammonia nitrogen at the carbonyl carbon and simultaneous proton transfer from ammonia to the substrate molecule. The latter, however, is transferred directly

DOI: 10.1039/b417285j

Table 1 Energy of transition states and intermediates relative to the reactants (in kcal mol^{-1}), and dipole moments μ (in D) in a vacuum

	HF[a]	B3LYP[b]	HF[c]	PCM_{Ac}[d]	PCM_{Ch}[d]	PCM_{H_2O}[d]	μ[e]	MP2[f]	E^g	E^{hf}
TS1-ph	56.5	41.0	56.9	54.3	55.5	53.2	4.29	35.6	32.9	
I-ph	7.4	6.9	9.0	8.6	9.0	8.3	2.43	−0.2	−0.6	
TS2-ph	36.5	24.5	33.7	28.4	30.3	23.1	6.97	24.9	19.6	25.1
TSc-ph	48.2	30.8	48.6	38.2	41.5	34.4	8.65	30.2	19.9	
Ph[i]	−2.8	−2.4	−5.7	−11.1	−9.9	−15.3		−3.9	−9.4	
TS1-cat1	55.4	39.2	63.0	57.5	59.5	56.6	6.78	41.8	36.2	
TS1-cat2	43.8	27.0	52.8	49.9	51.1	50.2	6.02	31.2	28.3	
TS2-cat	28.0	17.0	33.3	29.5	30.9	25.8	6.37	24.9	21.2	19.5
I-cat1	4.9	4.2	13.3	11.3	12.2	9.5	2.14	5.4	3.4	
I-cat2	−2.4	−3.4	6.6	5.7	6.2	5.9	3.07	−1.8	−2.7	
I-cat3	−2.1	−2.9	6.4	5.7	6.1	6.8	3.31	−1.9	−2.6	
I-cat4	3.5	2.2	11.7	9.6	10.5	9.5	4.02	3.1	1.0	
TSc-cat	39.8	21.5	46.6	37.1	39.9	32.9	9.71	28.0	18.5	
Cat[i]	−8.9	−8.4	−4.2	−10.4	−9.1	−16.7		−1.2	−7.5	
TS1-an	24.2	—	25.4	26.9	26.9	27.2	3.34	6.3	7.8	
I-an1	—	—	13.5	10.8	14.1	20.1	2.90	−0.2	−2.8	
I-an2	3.2	—	5.3	11.1	9.8	16.5	5.41	−8.0	−2.2	
I-an3	−1.2	−6.5	0.7	5.2	4.3	9.8	4.73	−10.4	−5.9	
I-an4	−1.3	−6.9	6.7	12.0	10.8	19.4	4.32	−2.9	2.3	
TS2-an	—	—	5.5	12.2	10.7	17.3	4.70	−7.9	−1.1	0.2
TSh-an	—	—	7.0	14.8	12.8	17.0	5.16	−9.0	16.8	
An[i]	−3.3	−6.5	−6.6	−8.9	−9.6	−5.3		−5.4	−7.7	

[a] HF/6-31G*. [b] B3LYP/6-31+G*. [c] HF/6-311++G**. [d] Single point PCM calculations at HF/6-311++G** level in corresponding solvent, acetonitrile, chloroform, or water. [e] Dipole moments μ obtained at HF/6-311++G** level. [f] MP2/6-311++G**//HF/6-311++G**. [g] MP2/6-311++G**//HF/6-311++G** with included solvation energy (acetonitrile). [h] Barrier of the reaction step at MP2/HF level, energy of second reaction barrier is calculated with respect to intermediate geometrically closest to TS2. [i] Calculated reaction energy for corresponding ammonolysis.

to the ester oxygen O_e, and is accompanied by simultaneous cleavage of the ester bond C–O_e resulting in one step formation of the products.[12]

Energies and activation barriers at different basis set and levels of calculation for the ammonolysis of acetylphenol, acetylcatechol and acetylcatechol monoanion are listed in Table 1. All energy variations discussed in the text are based on the results obtained at MP2/6-311++G**//HF/6-311++G** level since this is the highest computational level in our model study. In addition in parentheses we provide corresponding values at the HF level with the same basis set. Selected geometrical parameters of the transition states and intermediates discussed below are summarised in Table 2.

2.2 Ammonolysis of acetylphenol

The ammonolysis of acetylphenol was studied as a reference reaction in which no catalysis occurs. Calculations show that in the first transition state of the stepwise mechanism, **TS1-ph** (Fig. 1), the new N–C bond is almost formed and the former carbonyl carbon is close to tetrahedral. The former C=O_e bond is extended to 1.32 Å *vs.* 1.18 Å in acetylphenol. The proton to be transferred, however, is still closer to the ammonia nitrogen (1.20 Å) than to the former carbonyl oxygen O_e (1.32 Å). The proton transfer is difficult because of the relatively sharp N–H–O_e angle (115°), the optimal angle being in the range of 160°–180°.[13,14] The four atoms participating in this step (C_e, N, O_e, and ammonia H) are almost coplanar. On the other hand, the carbonyl carbon is out of the plane of the aromatic ring (the corresponding dihedral angle being 64°, Table 2) which prevents π-electron conjugation of the reaction centre with the aromatic ring.

In the intermediate **I-ph** the valence angles at the former carbonyl carbon atom are close to tetrahedral. The distance 2.15 Å between the proton of the newly formed O_eH group and the ester oxygen O_e suggests that they are connected by a weak hydrogen bond.

In the second transition state **TS2-ph**, the former ester bond is almost broken (bond length 2.27 Å) and the carbonyl carbon is almost planar, *i.e.*-product-like. The proton transfer, however, is in its initial stage since the length of the O_e–H bond to be broken is 0.99 Å, while that of the bond to be formed O_e–H is quite long (1.66 Å). The angle O_e–H–O_e associated with the proton transfer is larger (129°) than that (115°) in the **TS1-ph**, which probably facilitates the proton transfer and contributes to the decrease of **TS2-ph** energy. The breakdown of this transition state results in formation of the products (phenol and acetamide).

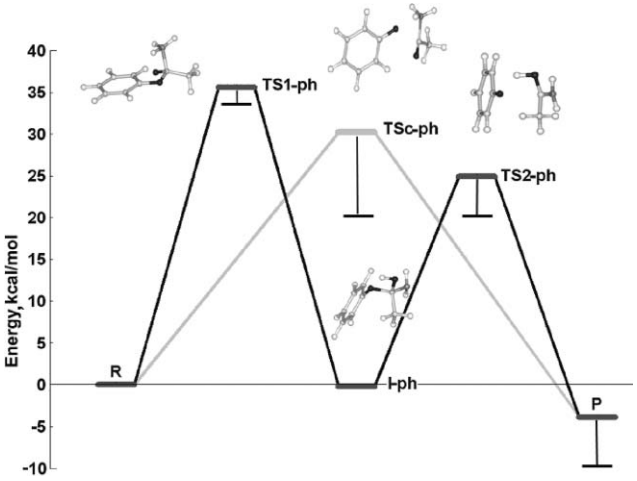

Fig. 1 Energy diagram of acetylphenol ammonolysis obtained at MP2/6-311++G**//HF/6-311++G** level. Stepwise mechanism is in black, concerted in grey, "R" and "P" represent energy of reactants and products, respectively. The energy shift due to solvent effect (acetonitrile) is shown by thin lines (see text for details).

The structure of the transition state for the concerted mechanism **TSc-ph** is similar to **TS2-ph** since the ester bond C–O_e is already broken (1.99 Å long) (Table 2), while the proton in flight is still bound to the ammonia molecule (N–H bond is 1.01 Å long). Although the length of the carbonyl bond C=O (1.18 Å) is close to the length of this bond in acetylphenol (1.19 Å), the formation of the new C–N bond is almost complete (bond length 1.56 Å) probably at the expense of the cleavage of the ester bond.

Table 2 Geometry parameters of transition states and intermediates for structures optimised at HF/6-311++G** level (bond lengths in Å, angles in degrees)

			Distances					Angles				Dihedral angles		
	HB[a]	HB[b]	C–Oe	C–O_c	C–N	N(O)–H[c]	H–O[d]	O–C–N(O)[e]	C–N(O)–H[f]	N(O)–H–O[g]	H–O–C[h]	Reac.[i]	**Ph**[j]	**cat**[k]
TS1-ph	—	—	1.40	1.32	1.56	1.20	1.32	95.02	72.26	115.3	77.33	1.12	64.03	—
I-ph	—	—	1.44	1.38	1.42	0.94	2.15	103.1	108.4	81.03	60.13	60.49	90.94	—
TS2-ph	—	—	2.27	1.30	1.30	0.99	1.66	79.65	100.2	129.1	50.53	4.21	82.99	—
TSc-ph	—	—	1.99	1.18	1.56	1.01	1.88	82.14	104.6	104.5	64.27	18.07	64.67	—
TS1-cat1	O_v–HN	2.24	1.42	1.32	1.54	1.20	1.33	95.73	72.43	114.5	76.97	5.17	85.04	9.56
TS1-cat2	O_vH–O_c	1.79	1.39	1.34	1.54	1.21	1.31	94.68	72.83	115.1	77.37	0.12	72.16	34.10
TS2-cat	O_v–HN	2.33	2.34	1.31	1.49	0.97	1.73	79.28	192.3	128.3	49.32	5.8	69.10	38.40
I-cat1	O_v–HN	2.33	1.45	1.38	1.42	—	—	—	—	—	—	63.23	74.99	1.82
I-cat2	O_vH–N	2.15	1.40	1.39	1.43	—	—	—	—	—	—	56.93	90.57	29.90
I-cat3	O_vH–O_c	1.94	1.40	1.40	1.43	—	—	—	—	—	—	162.9	86.38	23.90
I-cat4	Ov–HO_c	1.99	1.44	1.38	1.42	—	—	—	—	—	—	42.95	73.84	4.01
TSc-cat	O_vH–O_c	2.24	1.95	1.18	1.56	1.02	1.79	82.53	102.6	108.7	65.98	2.0	76.67	5.51
TS1-an	—	—	1.44	1.26	1.60	1.14	1.34	101.1	104.8	171.1	111.5	39.32	72.91	82.78
I-an1	O_vH–N	1.86	1.55	1.26	1.49	—	—	—	—	169.8	—	—	75.34	17.81
I-an2	O_vH–O_c	1.57	1.55	1.29	1.45	—	—	—	—	163.9	—	—	66.11	29.74
I-an3	O_v–HO	1.68	1.42	1.37	1.44	—	—	—	—	161.4	—	—	58.55	9.5
I-an4	O_v–HN	1.92	1.40	1.40	1.44	—	—	—	—	157.9	—	—	81.45	27.7
TS2-an	O_vH–O_c	1.65	1.67	1.29	1.43	—	—	—	—	163.7	—	—	65.30	30.66
TSh-an	—	—	1.47	1.32	1.45	1.23	1.14	—	111.2	172.5	—	—	58.33	20.37

[a] Shortest hydrogen bond in structure. [b] Length of shortest hydrogen bond including vicinal hydroxyl group, found in structure. [c] Distance between donor of proton to be transferred and proton. [d] Distance between acceptor of proton to be transferred and proton. [e] Angle between proton acceptor, carbonyl C atom and proton donor. [f] Angle between carbonyl C atom, proton donor and proton. [g] Angle between proton donor, proton and proton acceptor. [h] Angle between proton, proton acceptor and carbonyl C atom. [i] Dihedral angle: proton acceptor, carbonyl C atom, proton donor and proton to be transferred. [j] Dihedral angle between carbonyl group and benzene ring (O_c–C–O_e–C_{Ph} where C_{Ph} is the atom from the benzene ring attached to the vicinal oxygen). [k] Dihedral angle between vicinal hydroxyl group and benzene ring (H_v–O_v–$C^1{}_{Ph}$–$C^2{}_{Ph}$ where $C^1{}_{Ph}$ is the carbonyl atom from the benzene ring attached to the vicinal oxygen).

The angle associated with the proton transfer in this transition state is only 108°, resulting in the relatively high **TSc-ph** energy.

In the stepwise mechanism the energy of **TS2-ph** is 10.7 (23.2) kcal mol^{-1} lower than the energy of **TS1-ph** relative to the reactants and the second barrier is 10.5 (32.2) kcal mol^{-1} lower than the first barrier suggesting a rate limiting first step. Comparing results at MP2 and HF levels, one observes that the correlation effects reduce the energy difference between the two barriers almost twice, by 21.7 kcal mol^{-1} (Table 1). In general, the correlation effects reduce substantially the energy of all transition states and intermediates, but the relative order of stability is the same at HF, B3LYP, and MP2 levels of calculation. As seen in Fig. 1, the stability of the intermediate **I-ph** is similar to that of the reactants, and its energy is only 3.7 (14.7) kcal mol^{-1} higher than the energy of the products.

The calculations suggest that the reaction is slightly exothermic, the products being 3.9 (5.7) kcal mol^{-1} more stable than the reactants (the energies of separated molecules of reactants and products are considered). As seen, the **TS1-ph** transition state has the highest energy, which suggests that the reaction proceeds *via* a concerted mechanism, in which the barrier is 5.4 (8.3) kcal mol^{-1} lower than in the stepwise one.

2.3 Ammonolysis of acetylcatechol

The presence of an *o*-hydroxy group in acetylphenol provides additional possibilities for interactions between atoms in the reaction course. In most of the calculated structures, these interactions stabilise the transition states and the intermediates relative to the corresponding structures in the ammonolysis of acetylphenol.

We found two structures **TS1-cat1** and **TS1-cat2** (Fig. 2) for the first transition state of the stepwise mechanism. They are similar to **TS1-ph** but the second one is stabilised by hydrogen bonding between the *o*-OH proton H_v, and the carbonyl oxygen atom O_c, that is accepting the transferring proton from ammonia. This hydrogen bond is relatively short, 1.72 Å, providing one of the reasons for the 10.6 (10.2) kcal mol^{-1} lower energy of **TS1-cat2** (Table 1) compared to **TS1-cat1**. The former carbonyl C atom is close to tetrahedral in both structures suggesting late (intermediate-like) transition states.

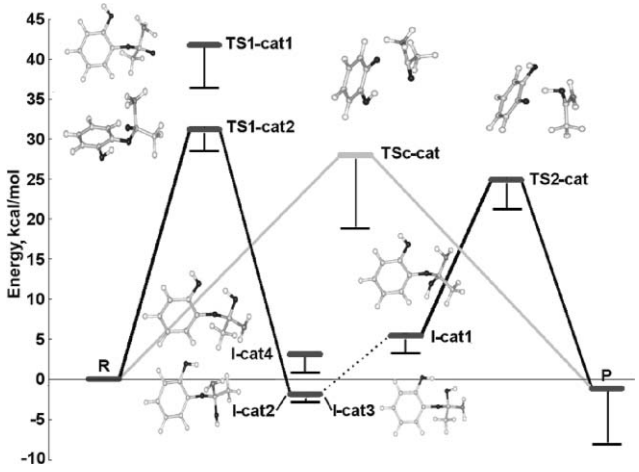

Fig. 2 Energy diagram of acetylcatechol ammonolysis obtained at MP2/6-311++G**//HF/6-311++G** level. The structures participating in the stepwise mechanism are shown in black. Dashed line corresponds to location of rotational barriers. Concerted mechanism is in grey. "R" and "P" represent energy of reactants and products, respectively. The energy shift due to solvent effect (acetonitrile) is shown by thin lines (see text for details).

The four-atom cycles in which the proton transfer occurs are planar with N–H–O_c angles close to the corresponding value for **TS1-ph**. The reaction centre is out of the plane of the aromatic ring (dihedral angles 72° and 85°), which prevents the interaction of the reaction centre with the aromatic π-electron system and a corresponding stabilisation of these transition states.

We found four structures **I-cat1**–**I-cat4** of the intermediate **I** that differ in the type of the hydrogen bonding interactions. In the conformers **I-cat1** and **I-cat2** the hydrogen bond is between the *o*-OH and the amino group, the latter acting as proton donor in **I-cat1** and proton acceptor in **I-cat2**. These hydrogen bonds are longer (2.33 and 2.15 Å, resp.) than the hydrogen bonds between the *o*-OH group and the newly formed hydroxyl group O_cH (1.94 and 1.99 Å) in the conformers **I-cat3** and **I-cat4**. When the vicinal hydroxyl is a proton donor, the intermediates (**I-cat2** and **I-cat3**) are more stable, reaction energies of −1.8 and −1.9 kcal mol^{-1} (Table 1), than the intermediates (**I-cat1** and **I-cat4**) with the vicinal hydroxyl acting as proton acceptor, reaction energies of 5.4 and 3.1 kcal mol^{-1} (Table 1). This is in agreement with the calculations of Ahn *et al.*[15] for hydrogen bonding ability of substituted phenols in complexes with water and with the known higher acidity and lower basicity of phenolic *vs.* alcoholic hydroxy groups. Due to conformational limitations, the angles between proton donor, proton and proton acceptor are not optimal for hydrogen bonding. They are in the range 132.1°–152.4°, while in unconstrained molecular complexes this angle is close to 180°.[13,14,16] The shortest hydrogen bond (1.94 Å) is found in the most stable conformation of the intermediate (**I-cat3**). When electron correlation effects are taken into account (at MP2 level), this conformation is 1.9 kcal mol^{-1} and 0.7 kcal mol^{-1} more stable than the reactants and the products, respectively.

Only one structure **TS2-cat** was obtained for the second transition state **TS2-cat** (Fig. 2) and it is very similar to that of **TS2-ph** (Fig. 1). The *o*-hydroxyl group contributes to the formation of two additional weak hydrogen bonds (2.33 and 2.43 Å long) acting as a proton acceptor for the amide group and a proton donor to the O_e. These interactions most likely facilitate O_e–C bond breaking and stabilise the transition state in which the distance between O_e–C_c is longer and the proton is less detached from O_c than in **TS2-ph**.

Only one structure was located and characterised as transition state of the concerted mechanism **TSc-cat** (Fig. 2). Although the interatomic distances around the reaction centre slightly differ from those of **TSc-ph** (Fig 1), the structures of both transition states are very similar (Table 2). There are two additional hydrogen bonds in **TSc-cat** between the *o*-OH group and the former carbonyl O_c and ester O_e oxygen atoms. They are, however, rather weak (2.44 Å and 2.24 Å long, respectively) resulting in its very small stabilisation (only 2.2 kcal mol^{-1}) relative to the reference transition state **TSc-ph**.

As can be seen in Fig. 2, the stability of the intermediates and the reactants is almost the same. Unlike acetylphenol ammonolysis, there are several structures of the intermediates of the stepwise mechanism with a maximal energy difference of 7.3 (6.9) kcal mol^{-1} depending on the hydrogen bonds formed. In general, the stability of the intermediates is close to that of the reactants and products. Moreover, the most stable intermediate structure, **I-cat3**, has a lower energy than the products, when calculated at the MP2 level. This is a result of the underestimation of the energy of the products, which is calculated for separated molecules (without hydrogen bonds), while hydrogen bonds contribute to the stabilisation of the intermediate. The contribution of a single H-bond between two neutral molecules is estimated to 6–9 kcal mol^{-1}.[13,14,17]

In the stepwise mechanism the second transition state is more stable than **TS1-cat**. The second barrier is 11.7 (32.8) kcal mol^{-1} lower than the first barrier, *i.e.* the first step is rate limiting. Correlation effects reduce substantially the energy of all transition states and of the intermediate but again they influence mainly the energy reduction of the first barrier (by 21.6 kcal mol^{-1}), while the energy of the second one remains unchanged. The relative order of stability is the same at HF, B3LYP and

MP2//HF levels. The energy difference between the products and reagents in acetylcatechol ammonolysis is 1.2 (4.2) kcal mol^{-1}, even smaller than in the case of acetylphenol (Table 1). In acetylcatechol ammonolysis, again, the concerted mechanism is the favoured one: **TSc-cat** is 3.2 (6.2) kcal mol^{-1} lower in energy than the more stable conformer of the first transition state of the stepwise mechanism **TS1-cat2**.

2.4 Ammonolysis of the acetylcatechol monoanion

As can be expected, due to the presence of a deprotonated hydroxyl group in the position vicinal to the reaction centre, the calculated transition states and intermediates for the ammonolysis of the acetylcatechol monoanion differ substantially from those of acetylphenol and acetylcatechol. As shown in Section 2.3, the intact *o*-OH group is a weaker proton acceptor than the carbonyl oxygen O_c and therefore it does not influence the reaction by direct detachment of the ammonia proton. In the case of a deprotonated *o*-OH (*o*-oxyanion), however, transition states involving proton transfer to the carbonyl O_c similar to **TS1-ph** and **TS1-cat**, were not found.

On the contrary, we found that in **TS1-an** (Scheme 2, Fig. 3) the proton from the attached NH_3 molecule is transferred to the adjacent phenolic oxyanion O_v that bears a considerably higher negative charge (−0.46 e) than O_c (−0.25 e) according to the Löwdin population analysis). In the transition state **TS1-cat** the charges are −0.43 e and −0.48 e, respectively. As in the other reactions, studied, in **TS1-an** the new C–N bond is essentially formed, but the distance C–N is longer (1.60 Å) and the proton is less detached, the new O_v–H bond is also substantially long, R(Ov–H) = 1.34 Å (Fig. 3 and Table 2). Therefore, the transition state is product-like with an almost tetrahedral hybridisation of the former carbonyl carbon. The ester group is again out of the plane of the aromatic ring, rotated at 73°. This transition state is considerably more stable than the corresponding transition states for the ammonolysis of acetylphenol or acetylcatechol (**TS1-ph**, **TS1-cat1** and **TS1-cat2**).

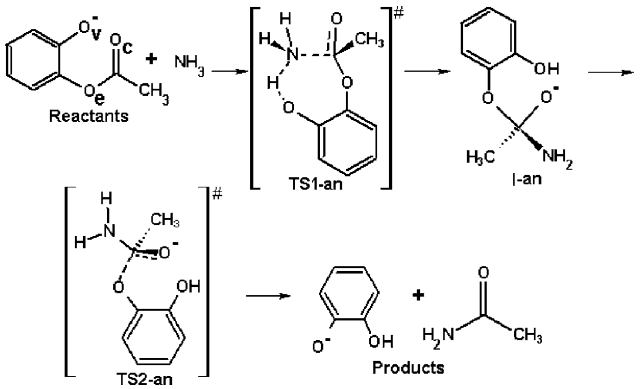

Scheme 2 Reaction mechanism for ammonolysis of acetylcatechol monoanion.

The stabilisation comes from the higher proton affinity of the anionic oxygen centre O_v of the ionised *o*-OH as compared to that of the carbonyl oxygen centre. Another feature of **TS1-an** is the almost linear position of the atoms participating in the proton transfer: the angle N–H_t–O_v is equal to 171°. Accordingly, such a linearity is assumed to facilitate the proton transfer[13,14] and contributes to the reduction of the activation energy for the reaction *via* **TS1-an**.

The intermediate **I-an1** is formed after association of ammonia with the carbonyl C atom and a proton transfer from ammonia to the anionic O_v centre (Fig. 3). As seen from Scheme 2, the negative charge in this intermediate is located mainly on the former carbonyl oxygen O_c. The *o*-OH group is hydrogen bonded to the amino group nitrogen, the H_v–N

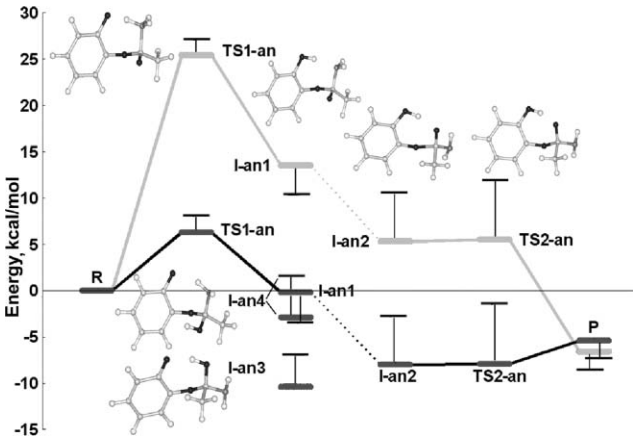

Fig. 3 Energy diagram of acetylcatechol monoanion ammonolysis. Calculations at MP2/6-311++G**//HF/6-311++G** and HF/6-311++G** levels in black and in grey, respectively. Dashed line represents section where rotational barrier is located. The energy shift due to solvent effect (acetonitrile) is shown by thin lines (see text for details).

distance being equal to 1.86 Å. A rotation around the ester bond O_e–C, results in a more stable conformer of the intermediate **I-an2**, where the hydrogen bond is between the *o*-O_vH group and the anionic O_c centre. Due to the negative charge of the O_c centre in **I-an2**, an intramolecular proton transfer can occur leading to a new intermediate **I-an3**, where the *o*-OH is again deprotonated as in the initial substrate and a new O_cH group is formed. The transition between the intermediates **I-an3** and **I-an2** goes through a transition state **TSh-an** with low activation energy, 1.4 (6.3) kcal mol^{-1} (not shown in Fig. 3), *i.e.* the proton exchange between O_v and O_c oxygen centres occurs easily and most likely the two forms of the intermediate are in equilibrium with a slight domination of **I-an3** that is 2.4 (4.6) kcal mol^{-1} more stable than **I-an2**.

The structure **I-an3**, in which the negative charge is on the O_v oxygen centre, is the most stable structure of the intermediate probably because of the partial redistribution of the negative charge from the O_v centre in the aromatic ring. On the other hand, in **I-an2** the negative charge is essentially localised on the former carbonyl oxygen, O_c. The intermediate **I-an3** can be transformed after rotation around the ester bond to a new structure (**I-an4**) with a hydrogen bond between the NH_2 group and the anionic oxygen centre O_v. This hydrogen bond, however, is relatively weak, R(H–O_v) = 1.92 Å, and the structure is less stable than the other structures of intermediate **I**. The intermediates in which *o*-OH is deprotonated are more stable due to the negative charge delocalisation in the aromatic ring. Among all four structures of the intermediate, only the intermediate **I-an1** can be transformed into products, *via* the transition state **TS2-an**. In the force constant matrix of this transition state there is one low negative value that corresponds to the bond between the ester oxygen atom O_e and the former carbonyl carbon atom. One can expect that such a C–O bond cleavage would proceed with continuous increase in the energy of the system without a clear maximum, because of the relatively high energy for cleavage of the O_e–C single bond as compared to forming a second O_c–C bond. Due to the presence of the hydrogen bond between the carbonyl O_c atom and the *o*-OH, however, we found an energy maximum (transition state **TS2-an**) when the calculations were performed at the HF level. The energy of this structure, **TS2-an**, calculated at the MP2 level is between the energies of the intermediate **I-an1** and the separated products. One could even expect an absence of **TS2-an** due to the well-known lack of a transition state during anionic attack at a carbonyl carbon atom in the gas phase.[18–20]

We did not find any transition state similar to **TSc-ph** and **TSc-cat** for the concerted mechanism most probably because of

the presence of the adjacent negative charge on the *o*-oxyanion that strongly attracts the proton to be transferred.

The separated products are 5.4 (6.6) kcal mol^{-1} more stable than the reactants (Table 1). The lower energy of the intermediate **I-an2** and **I-an3** in the gas phase compared to the energy of the products is presumably due to the hydrogen bond that is not taken into account for the separated products. The energy of **TS2-an** is much lower than that of **TS1-an**. Therefore, the activation barrier for the ammonolysis of the acetylcatechol monoanion is controlled by the energy of the first transition state **TS1-an**.

2.5 Solvent effect

In order to understand the medium effect on the reaction energetics we carried out polarised continuum model (PCM) calculations for three different solvents at HF/6-311++G** level. Previous theoretical study of methyl formate ammonolysis[11] has shown that the solvent effect obtained by optimisation of the pertinent structures in solvent (acetonitrile) changes synchronously the energies of intermediates and transition states along the reaction path. In addition, the recent computational study of Lithoxoidou and Bakalbassis[21] suggested that the presence of solvent (accounted for by PCM) influences the interatomic distances in various aromatic compounds by less than 0.004 Å for solvents with $\varepsilon < 37$, and at most 0.014 Å for more polar solvents, like methanol and water, while the changes of the bond angles are below 1.5 degrees. On the basis of such observations we evaluated the solvent effect in a single-point fashion using the gas phase geometry of the structures optimised at the same computational level. Such an approach is often applied for the evaluation of the influence of different solvents on various organic reactions.[22,23] We used acetonitrile, chloroform and water to cover different parts of the dielectric constant scale.

The calculated values are reported in Table 1 and corresponding energy shifts due to solvent effect contribution evaluated at HF/6-311++G** level in acetonitrile are shown in Figs. 1–3. The results suggest that the presence of a solvent lowers all barriers both for acetylphenol and acetylcatechol ammonolysis (Figs. 1, 2). This effect could be attributed to the generation of a mirror charge in the solvent in the case of intermediates and transition states because of their larger localised charges in the reaction centre. As expected, the stabilisation of the transition states in general correlates with their polarity estimated by the dipole moments of the species (Table 1). Indeed, both **TSc-ph** and **TSc-cat** transition states have high dipole moments, above 10 D, and the corresponding stabilisation due to the presence of solvent is 6.7–14.2 kcal mol^{-1} for the modelled solvents. The intermediates feature low dipole moments, at most 4.0 D, and their solvent effect stabilisation is much lower, between zero and 3.8 kcal mol^{-1}. This gives rise to stabilisation of the intermediate species with respect to the reactants and to a corresponding lowering of the reaction barriers. Furthermore, the energy barriers decrease with increasing the dielectric constant of the solvent in the order vacuum > chloroform > acetonitrile > water. The solvent affects the transition states energy of the concerted mechanism and the second transition state of the stepwise mechanism. The concerted reaction path remains the most favourable and the first barrier of the stepwise mechanism remains higher than the second one as found from the calculations in vacuum. This is in accord with the results of Ilieva *et al.*[11] that modelled the reactions of methyl formate and ammonia using PCM with acetonitrile as solvent.

In the case of the acetylcatechol-monoanion ammonolysis, however, the solvent effect leads to the opposite tendency—energy barriers increase with increasing the dielectric constant; *i.e.* the lowest energy barriers are in vacuum. As seen in Scheme 2, the charged species in this reaction are the initial acetylcatechol monoanion and the product (catechol monoanion), where the *o*-oxygen centre O_v is anionic. For this reason the presence of solvent leads to stabilisation of the charged reactants as compared to the intermediates and transition states, which effectively increases the reaction barriers. Even with this increase (by 1.5 kcal mol^{-1}), the reaction barrier for the ammonolysis of the acetylcatechol monoanion remains substantially lower than that of acetylphenol and acetylcatechol ammonolysis, by 11.3 and 10.2 kcal mol^{-1} respectively. Unlike acetylphenol and acetylcatechol ammonolysis, the solvent effect on the reaction with ionised acetylcatechol does not correlate with the dipole moments of the intermediate species.

3 Discussion

The preferred reaction mechanism for acetylphenol and acetylcatechol aminolysis is the concerted mechanism with reaction barriers 30.2 and 28.0 kcal mol^{-1} calculated at the MP2//HF level. The presence of *o*-OH group in acetylcatechol stabilises slightly, by 4.4 (4.1) kcal mol^{-1}, the first transition state of the stepwise mechanism **TS1-cat** *vs.* **TS1-ph**, while the stabilisation of the transition state for the concerted mechanism **TSc-cat** is two times smaller, by 2.2 (2.0) kcal mol^{-1}. The stabilisation of **TS1-cat2** relative to **TS1-cat1** is 10.6 (10.2) kcal mol^{-1}. This can be attributed to differences in the mode of hydrogen bonding since there are similar hydrogen bonds in **I-cat1** and **I-cat3** with similar energy difference, 7.3 (6.9) kcal mol^{-1}, the largest among **I-cat** intermediates.

As seen from the calculated structures (Figs. 2, 3), the hydrogen bonds with the neighbouring intact or deprotonated *o*-OH group play an important role in the stabilisation of both transition states and intermediates. These intramolecular hydrogen bonds, however, can be catalytically important only when they are stronger in the transition state than in the reactants and intermediates.

It is universally acknowledged that the strength of the hydrogen bond strongly depends on the charge of the proton acceptor and, particularly in this case, on the charge of the anionic proton acceptor. The energy of the hydrogen bond in H–O–H $\cdots$ neutral molecule (Ph–OH) is about 5.5 kcal mol^{-1}, 19.9 kcal mol^{-1} in H–O–H $\cdots$ $^{-}$OCH$_3$ and 23.3 kcal mol^{-1} in H–O–H $\cdots$ F^{-}.[24] Based on atomic charges obtained by Löwdin analysis, this tendency is observed in our results as well. The charges of the proton acceptors (O_v or O_c) in hydrogen bonds in transition states **TS1-cat1**, **TSc-cat** and **TS1-cat2** are −0.17 e, −0.26 e and −0.44 e, respectively, while in acetylcatechol the charge of the proton acceptor is −0.26 e. The larger negative charge on O_c is due to the semi-cleaved double C–O_c bond in **TS1**. The strongest catalytic effect is observed for the transition states of the acetylcatechol anion, where the strongest hydrogen bond is formed due to the negative charge on the proton accepting oxygen centres. The lower catalytic effect of the H-bonded *o*-OH group in the concerted mechanism can be attributed to the steric hindrance of hydrogen bonding in the transition state **TSc-cat**.

While the ammonolysis mechanisms of acetylphenol and acetylcatechol, predicted by calculations are very similar, the energy profile for the ammonolysis of the acetylcatechol monoanion differs considerably. In this case a kind of stepwise mechanism is preferred, but the proton acceptor is the vicinal anionic oxygen centre due to the higher basicity of O_v as compared to the other oxygen atoms in the structures. The presence of a negative charge gives rise to a considerable stabilisation of the transition state: the energy of **TS1-an** is 29.3 (31.5) and 24.9 (27.4) kcal mol^{-1} lower than that of the transition states **TS1-ph** and **TS1-cat2**. The presence of an adjacent negatively charged oxygen (a deprotonated vicinal hydroxyl group), promotes a decrease of the energy of the intermediate **I-an3**. Although to a lower extent, 10.2 (8.3) kcal mol^{-1} relative to that of acetylphenol, it is promoted by the hydrogen bonding to negatively charged proton acceptors as well.

Our results suggest that the resonance influence of the *o*-OH group on the transition states can be neglected. All the transition states found, are late, with hybridisation of the carbonyl carbon atom close to sp^3, which practically excludes its conjugation with the π-electrons of the aromatic ring. Furthermore, the large torsion angle between the plane of the aromatic ring and the $C–O_c$ bond between the carbonyl carbon and the carbonyl oxygen prevents the π-electron interaction with the aromatic electron system. Therefore, the results obtained for acetylcatechol ammonolysis could be extrapolated to a plausible mechanism of the peptidyl tRNA aminolysis assisted by its 3′-terminal adenosine 2′-OH.

The calculations demonstrate that both the intact and the ionised *o*-OH group promote anchimeric catalysis[25] of acetylcatechol ammonolysis. The nonionised *o*-OH group lowers the rate-limiting reaction barrier by 2.2 (2.0) kcal mol^{-1}. A dramatic increase of the reaction rate and a change of the reaction mechanism, however, can be expected when the *o*-OH group is ionised. The decrease of the activation energy in this case is 21.7 (21.2) kcal mol^{-1} relative to that of the neutral *o*-OH group and 23.9 (23.2) kcal mol^{-1} relative to the *o*-deoxysubstrate (acetylphenol).

The solvent effect study shows that in the case of an intact *o*-OH group the solvent substantially lowers all reaction barriers but the relative order of the competing reaction paths remains similar (Figs. 1, 2). In the case of an ionised *o*-OH group the solvent slightly increases the energy barriers for the stepwise mechanism but the first barrier remains higher than the second one. Despite this unfavourable solvent effect, the decrease of the activation energy is still 10.2 kcal mol^{-1} lower relative to the ammonolysis of the substrate with intact *o*-OH (acetylcatechol) and 11.3 kcal mol^{-1} lower relative to the *o*-deoxysubstrate (acetylphenol).

4 Conclusions

The computational modelling of the *o*-OH effect on the ammonolysis of acetylphenol resulted in reaction energy barriers of 30.2 kcal mol^{-1} for the *o*-deoxy and 28.0 kcal mol^{-1} for the *o*-hydroxysubstrates. Deprotonation of the *o*-hydroxyl group leads to an even stronger lowering of the activation energy to 6.3 kcal mol^{-1}. These results suggest that the intramolecular *o*-oxyanion-catalysed ammonolysis of acetylcatechol is orders of magnitude faster than the uncatalysed reaction or the reaction catalysed by the nonionised *o*-OH group. An analogy with the aminolysis of peptidyl tRNA implies orders of magnitude acceleration of protein biosynthesis after ionisation of its 3′-terminal adenosine 2′-OH. Therefore, even partial deprotonation of this 2′-OH would provide a dominant substrate-assisted catalytic mechanism of the ribosome.

5 Computational details

Molecular orbital calculations were carried out by using the GAMESS Version 6[26] and GAUSSIAN98W[27] program suites. Analytical gradient optimisation methods were used to locate the minima, corresponding to reactants, intermediates and products, and saddle points corresponding to transition states. The calculations were performed at several levels, HF level with 6-31G*[28] and 6-311++G**[29] basis sets and B3LYP[30] level with 6-31+G*[28a–d] basis set. The geometries of all stationary points are optimised at HF/6-31G*, B3LYP/6-31+G* and HF/6-311++G** levels. Single point calculations at MP2[31,32] level with 6-311++G**[29] basis set on geometries optimised at HF/6-311++G** level are carried out in the attempt to refine the reaction energetics. Transition states were identified by finding only one negative eigenvalue of the analytic force constant matrix and by geometric analysis of its eigenvector components. The solvent effects were evaluated by the polarised continuum model (PCM)[33] as included in GAUSSIAN98 program. Single point PCM calculations at HF/6-311++G** level were performed for refining the energy changes of all stationary points along the modelled rate-determining reaction paths. We used standard dielectric constants implemented in GAUSSIAN98 for the solvents used. The energies of all structures are calculated with respect to the sum of the energies of corresponding reactants molecules considered as separated. The reaction energies are considered as a sum of the energies of the separated product molecules. The activation barriers of the **TS1** and **TSc** transition states are calculated with respect to the reactants, while the activation barriers of **TS2** are calculated with respect to the intermediate, which is geometrically closest to the **TS2**.

Acknowledgements

The authors are grateful to the Alexander von Humboldt Foundation

References

1 R. Mei and D. Herschlag, *Biochemistry*, 1996, **35**, 5796.
2 D. N. Wilson and K. H. Nierhaus, *Angew. Chem., Int. Ed. Engl.*, 2003, **42**, 3464.
3 K. H. Nierhaus, H. Schulze and B. S. Cooperman, *Biochem. Int.*, 1980, **1**, 185.
4 J. H. Jones and G. T. Young, *Chem. Commun.*, 1967, 35.
5 D. S. Kemp and S. W. Chien, *J. Am. Chem. Soc.*, 1967, **89**, 2743.
6 G. Ivanova, E. Bratovanova and D. D. Petkov, *J. Pept. Sci.*, 2002, **8**, 8.
7 A. Sievers, M. Beringer, M. V. Rodnina and R. Wolfenden, *Proc. Natl. Acad. Sci. USA*, 2004, **101**, 7897.
8 J. De Jersey, A. K. Fihelly and B. Zerner, *Bioorg. Chem.*, 1980, **9**, 153.
9 F. Menger and J. Smith, *J. Am. Chem. Soc.*, 1972, **94**, 3824.
10 J. Jensen, K. Baldridge and M. Gordon, *J. Phys. Chem.*, 1992, **96**, 8340.
11 S. Ilieva, B. Galabov, D. Musaev, K. Morokuma and H. Schaefer, *J. Org. Chem.*, 2003, **68**, 1496.
12 The carbonyl carbon atom is prohiral and after nucleophile attack of ammonia a chiral intermediate is formed, *i.e.* two reaction paths with *R* or *S* intermediates are possible. However, both reaction paths are energetically equivalent and we consider only the pro *S* attack and *S* configuration of the intermediates.
13 M. Buck and M. Karplus, *J. Phys. Chem. B*, 2001, **105**, 11000.
14 B. A. Grzybowsky, A. V. Ishchenco, R. S. DeWitte, G. M. Whitesides and E. I. Shakhnovich, *J. Chem. Phys. B*, 2000, **104**, 7293.
15 D. Ahn, S. Park and S. Lee, *J. Phys. Chem. A*, 2003, **107**, 131.
16 A. Abcowicz-Bienko and Z. Latajka, *J. Phys. Chem. A*, 2000, **104**, 1004.
17 R. Vargas, J. Garza, R. Friesner, H. Stern, B. Hay and D. Dixon, *J. Phys. Chem. A*, 2001, **105**, 4963.
18 J. Madura and W. Jorgensen, *J. Am. Chem. Soc.*, 1986, **108**, 2517.
19 S. Weiner, C. Singh and P. Kollman, *J. Am. Chem. Soc.*, 1985, **107**, 2219.
20 D. Bakowies and P. Kollman, *J. Am. Chem. Soc.*, 1999, **121**, 5712.
21 A. T. Lithoxoidou and E. G. Bakalbassis, *J. Phys. Chem. A*, 2005, **109**(2), 366.
22 (*a*) S. Ilieva, B. Galabov, D. Musaev and K. Morokuma, *J. Org. Chem.*, 2003, **68**, 3406; (*b*) N. Diaz, D. Suarez and T. L. Sordo, *J. Org. Chem.*, 1999, **64**, 3281.
23 E. A. Ivanova, Ph. Gisdakis, V. A. Nasluzov, A. I. Rubailo and N. Rösch, *Organometallics*, 2001, **20**, 1161.
24 L. Remer and J. Jensen, *J. Phys. Chem. A*, 2000, **104**, 9266.
25 P. Carter and W. Dall'Acqua, *Protein Sci.*, 2000, **9**, 1.
26 M. W. Schmidt, K. K. Baldridge, J. A. Boatz, S. T. Elbert, M. S. Gordon, J. H. Jensen, S. Koseki, N. Matsunaga, K. A. Nguyen, S. J. Su, T. L. Windus, M. Dupuis and J. A. Montgomery, *J. Comput. Chem.*, 1993, **14**, 1347.
27 M. J. Frisch, G. W. Trucks, H. B. Schlegel, G. E. Scuseria, M. A. Robb, J. R. Cheeseman, V. G. Zakrzewski, J. A. Montgomery, R. E. Stratmann, J. C. Burant, S. Dapprich, J. M. Millam, A. D. Daniels, K. N. Kudin, M. C. Strain, O. Farkas, J. Tomasi, V. Barone, M. Cossi, R. Cammi, B. Mennucci, C. Pomelli, C. Adamo, S. Clifford, J. Ochterski, G. A. Petersson, P. Y. Ayala, Q. Cui, K. Morokuma, D. K. Malick, A. D. Rabuck, K. Raghavachari, J. B. Foresman, J. Cioslowski, J. V. Ortiz, B. B. Stefanov, G. Liu, A. Liashenko, P. Piskorz, I. Komaromi, R. Gomperts, R. L. Martin, D. J. Fox, T. Keith, M. A. Al-Laham, C. Y. Peng, A. Nanayakkara, C. Gonzalez,

M. Challacombe, P. M. W. Gill, B. G. Johnson, W. Chen, M. W. Wong, J. L. Andres, M. Head-Gordon, E. S. Replogle, and J. A. Pople, GAUSSIAN98, Gaussian, Inc., Pittsburgh PA, 1998.
28 (*a*) R. Ditchfield, W. J. Hehre and J. A. Pople, *J. Chem. Phys.*, 1971, **54**, 724; (*b*) W. J. Hehre, R. Ditchfield and J. A. Pople, *J. Chem. Phys.*, 1972, **56**, 2257; (*c*) P. C. Hariharan and J. A. Pople, *Mol. Phys.*, 1974, **27**, 209; (*d*) M. S. Gordon, *Chem. Phys. Lett.*, 1980, **76**, 163; (*e*) P. C. Hariharan and J. A. Pople, *Theor. Chim. Acta*, 1973, **28**, 213–29.
29 (*a*) K. Raghavachari, J. A. Pople, E. S. Replogle and M. Head-Gordon, *J. Phys. Chem.*, 1990, **94**, 5579; (*b*) M. J. S. Dewar and C. H. Reynolds, *J. Comput. Chem.*, 1986, **2**, 140.
30 (*a*) A. D. Becke, *J. Chem. Phys.*, 1993, **98**, 5648; (*b*) C. Lee, W. Yang and R. G. Parr, *Phys. Rev. B*, 1988, **37**, 785.
31 J. A. Pople, J. S. Binkley and R. Seeger, *Int. J. Quantum Chem.*, 1976, **S10**, 1.
32 M. J. Frisch, M. Head-Gordon and J. A. Pople, *Chem. Phys. Lett.*, 1990, **166**, 275.
33 (*a*) S. Miertus, E. Scrocco and J. Tomasi, *Chem. Phys.*, 1981, **55**, 117; (*b*) S. Miertus and J. Tomasi, *Chem. Phys.*, 1982, **65**, 239; (*c*) M. Cossi, V. Barone, R. Cammi and J. Tomasi, *Chem. Phys. Lett.*, 1996, **255**, 327; (*d*) M. T. Cances, V. Mennucci and J. Tomasi, *J. Chem. Phys.*, 1997, **107**, 3032; (*e*) V. Barone, M. Cossi, B. Mennucci and J. Tomasi, *J. Chem. Phys.*, 1997, **107**, 3210; (*f*) M. Cossi, V. Barone and J. Tomasi, *Chem. Phys. Lett.*, 1998, **286**, 253; (*g*) V. Barone, M. Cossi and J. Tomasi, *J. Comput. Chem.*, 1998, **19**, 404; (*h*) V. Barone and M. Cossi, *J. Phys. Chem. A*, 1998, **102**, 1995; (*i*) B. Mennucci and J. Tomasi, *J. Chem. Phys.*, 1997, **106**, 5151.